Journal of
Marine Science and Engineering

MDPI

Article

An Operational Wave System within the Monitoring Program of a Mediterranean Beach

Andrea Ruju *,†, Marinella Passarella, Daniele Trogu, Carla Buosi, Angelo Ibba and Sandro De Muro

Department of Chemical and Geological Sciences, University of Cagliari, Cittadella Universitaria, 09042 Monserrato (CA), Italy; marinella.passarella@unica.it (M.P.); daniele.trogu@outlook.com (D.T.); cbuosi@unica.it (C.B.); aibba@unica.it (A.I.); demuros@unica.it (S.D.M.)

* Correspondence: rujua@unica.it; Tel.: +39-070-6757778

† Current address: France Energies Marines, Bâtiment Cap Océan, Technopôle Brest Iroise, 525 Avenue Alexis de Rochon, 29280 Plouzané, France

Received: 20 December 2018; Accepted: 30 January 2019; Published: 2 February 2019

Abstract: This work assesses the performance of an operational wave system in the Mediterranean Sea by comparing computed data with measurements collected at different water depths. Nearshore data measurements were collected through a field experiment carried out at Poetto beach (Southern Sardinia, Italy) during spring 2017. In addition to coastal observations, we use intermediate and deep water wave data measured by two buoys: one situated North-West of Corsica and the other in the Gulf of Lion. The operational wave system runs once a day to predict the wave evolution up to five days in advance. We use a multi-grid approach in which a large grid extends over the entire Mediterranean basin and a fine grid covers the coastal seas surrounding the islands of Sardinia and Corsica. The comparison with measurements shows that the operational wave system is able to satisfactorily reproduce the wave evolution in deep and intermediate waters where the relative error of the significant wave height is 17%. The error exceeding 25% in coastal waters suggests that the use of a finer grid and the coupling with an atmospheric model able to catch local effects is advisable to accurately address nearshore wave processes driven by coastal wind forcing.

Keywords: operational system; wave forecast; wave modelling; Mediterranean Sea; monitoring program; beach management

1. Introduction

The growing importance of economic activities in coastal areas highlights the need for the development and implementation of monitoring programs as a support for management and coastal hazard assessment. In this context, remote and in situ observations allow the monitoring of deep water and coastal dynamics and provide crucial data to track their evolution [1]. However, measurements have two main downsides: first, they usually lack large spatial coverage since data are available at specific locations and in the second place they are unable to foresee evolutions beyond the time of the latest measurement. Operational wave systems based on forecast simulations are able to predict wave conditions a few days in advance and provide conditions over a wide geographical area, thus extending and complementing the information from measurements [2]. Nowadays, monitoring programs including the combination of measurements and simulations seem to represent the best choice in terms of data reliability, spatial/time coverage and costs [3]. For this reason they continue to receive an increasing attention from coastal scientists and managers, providing benefits for beach management, risk assessment and coastal planning [4–6].

In this work, we assess the performance of an operational wave system in the Mediterranean Sea by comparing computed wave data with three measured wave datasets, one of them obtained in the nearshore and the others in intermediate and deep waters. The nearshore data were collected in the Gulf of Cagliari, Southern Sardinia, where this study focuses. In recent decades, the coastal areas of the Gulf of Cagliari have been experiencing an intense urbanization with the development of the city of Cagliari and its hinterland (about 500,000 inhabitants). Residential development in addition to industrial activities have led to significant human pressure on the two beach systems, Giorgino and Poetto, included in the metropolitan area of Cagliari. A monitoring program, including periodic field surveys and video image acquisition, has been set up and implemented in the last five years at Poetto beach by the Coastal and Marine Geomorphology Group (CMGG) of the University of Cagliari [7].

As a specific task of the beach monitoring program, a field experiment was carried out in spring 2017 to collect nearshore wave and current data. We use these nearshore data, together with intermediate and deep water buoy data proceeding from the French agencies Cerema and Meteo France, to assess the reliability of an operational wave system running for the entire duration of the experiment. A spectral wave model coupled with an atmospheric model is used to simulate wave propagation over the Mediterranean Sea, with an increased spatial resolution in the coastal waters surrounding the islands of Sardinia and Corsica. This operational wave system, replicable in similar contexts, can serve as a key tool for decision makers and stakeholders in various coastal and maritime sectors. For example, the maritime transport needs accurate wave forecasts in order to secure operations at sea and prevent potential pollution. Moreover, a detailed wave information is valuable to predict vulnerability to storm impacts including flooding risk. For instance, widely-used formulations for maximum runup prediction on beaches rely upon incoming wave parameters measured or computed in coastal waters outside the surf zone [8,9]. Thus, wave operational systems appear to be of importance for port authorities, civil protection and coastal managers to anticipate and respond to extreme wave conditions that could interfere in port operations or damage beach infrastructures, potentially leading to safety risks. Another important application concerns scientific and economic aspects linked to the coastal and marine planning projects, operational assistance in coastal development, and monitoring of coastal processes such as beach erosion and sediment transport.

The ultimate goal of this work is to test the viability of incorporating an operational wave system in a beach monitoring program for a Mediterranean urban beach, including remote as well as in situ measurements. Besides, our work aims to extend the current knowledge of the capabilities of operational wave systems in forecasting wave conditions in the Mediterranean Sea. In this study, special attention is devoted to the identification of the model limitations in reproducing coastal wave conditions generated over limited Mediterranean fetches (on the order of hundreds of km) and under the local influence of varying sea breezes. Wave modelling under these environmental conditions has been recognized as particularly challenging by the literature [10,11], thus requiring further research.

The paper is structured as follows. Section 2 describes the monitoring program along with the operational wave system. Section 3 reports the system validations against measured data. Section 4 discusses the results and Section 5 draws some conclusions.

2. Study Area and Methods

2.1. Study Area

Giorgino and Poetto beaches are located in the innermost part of the Gulf of Cagliari, respectively, west and east of the metropolitan area of Cagliari. Recent economic development (with the coexistence of industrial, fishing, touristic and recreational activities) has increased the vulnerability of Giorgino and Poetto beaches to coastal risks and in particular to flooding and erosion. For this reason, these microtidal wave-dominated beaches have been extensively studied through the BEACH (Beach Environment, management And Coastal Hazard) [7,12] and NEPTUNE (Natural Erosion Prevision Through Use of Numerical Environment) [13] projects carried out since 2013 by the Coastal and Marine Geomorphology

Group (CMGG) of the University of Cagliari. De Muro et al. [14] presented an integrated sea-land approach for mapping sedimentological processes of Poetto beach; whereas the geomorphological processes and anthropogenic modifications at Giorgino beach were studied by De Muro et al. [13].

Giorgino beach is an 11 km long embayment where the residential development has modified the coastal morphology and the fluvial system. The presence of industrial and port activities (such as dredging, dumping, movement of ships, anchorages, loading berths, fishing, discharge of untreated sewage) has been identified as the main cause of turbidity, pollution, toxicity and erosion [13]. Poetto beach is an urban sandy beach with a length of 8 km and a maximum width of about 100 m; it is the most populated beach in Sardinia (about 100,000 visitors per day in the summer [15]). See Figure 1 that displays a view of a moderate swell on Poetto beach from the video camera system installation. A nourishment project was carried out in 2002 on the western side of the beach area. The nourishment has significantly modified the textural, compositional and morphological features of the backshore, shoreline and shoreface [14]. Besides the mentioned beach nourishment, the intensification of anthropic pressure through an increasing number of residential users and tourists together with frequent beach cleaning operations (e.g., removal of seagrass berm) and other maintenance procedures (e.g., bulldozing) have a significant impact on the beach system affecting beach morphodynamic processes.

Figure 1. Snapshot of the Poetto beach captured by the video camera system during the moderate swell (significant wave height H_s = 1.27 m) occurred on 26 April 2017.

2.2. The Monitoring Program

The project NEPTUNE, led by the University of Cagliari, aimed at providing support for coastal management through the set-up of a monitoring program to track the main processes of the beach systems included in the metropolitan area of Cagliari. The measurements involved periodic topographic and bathymetric surveys, seabed quality assessment through bioindicators [16,17] and hydrodynamic observations. Due to the recognized importance of seagrasses in the mitigation of flood and erosion risks in microtidal Mediterranean beaches [18–20], special attention was devoted to the relationship between wave hydrodynamics and spatial distribution of the meadow of the endemic Mediterranean seagrass *Posidonia oceanica* [21,22]. Moreover, a video camera system was implemented to monitor coastal processes of Poetto beach including, for instance, beach morphodynamics and wave runup [23] and for the assessment of human impacts (especially beach cleaning and bulldozing). The video system application, operative nowadays, allows the observation of a broad range of nearshore hydrodynamic and morphological processes in support of coastal management and engineering [24,25]. Video monitoring techniques offer the chance to provide detailed coastal state information with high resolution in time and space in a relatively cheaper and safer way than deploying in situ instruments [24]. Through this system, it is also possible to provide direct support to coastal

managers. In addition, video images can integrate a warning system for forecasting beach flooding, in order to prevent the damage of coastal infrastructures [26].

2.3. Field Wave Data

Field measurements were carried out over a 6-week period at Poetto beach, from 30 March to 16 May 2017. Presented within this work are data collected by an Acoustic Wave And Current (AWAC) profiler deployed in the nearshore at a water depth of 18 m. The deployment location was chosen by scuba divers in a sandy intramatte region between patches of *Posidonia oceanica* meadow. The AWAC profiler measured directional spectra and bulk wave parameters with a time interval of two hours with the purpose of synchronizing incoming wave data with video data from the video camera system located on land (see Figure 1). The spectral estimates were obtained by applying Fourier transforms of time series of 1024 s sampled at 2 Hz. Besides marine data, a meteorological station located on land in the proximity of the beach recorded wind speed and other atmospheric variables. Readers are referred to Passarella [23] to obtain more details about this experiment.

In addition to coastal observations, we present here wave data measured by two wave buoys: one located in intermediate depths and the other moored in deep waters. Since during the period of the experiment there was no availability of measurements from wave buoys located in the vicinity of Sardinian coasts, we used data from the French network. The buoy located in intermediate waters is La Revellata directional buoy (managed by Cerema) that is moored in 130 m depth in the sea North-West of the island of Corsica (42.57° N, 8.65° E). Since at this water depth the low-frequency band of the wave spectrum ($f < 0.8$ Hz) is affected by the bottom, we refer to this buoy as located in intermediate water depths. The deep water device is an omnidirectional wave buoy managed by Meteo France. It is located in the Gulf of Lion (42.06° N, 4.64° E) in approximately 2300 m depth. It collects bulk wave parameters (significant wave height and period) every hour. Moreover, the buoy is equipped with an anemometer that measures wind speed and wind direction at 3 m above the sea level. Figure 2 shows the geographic setting with the locations of the two wave buoys and the AWAC.

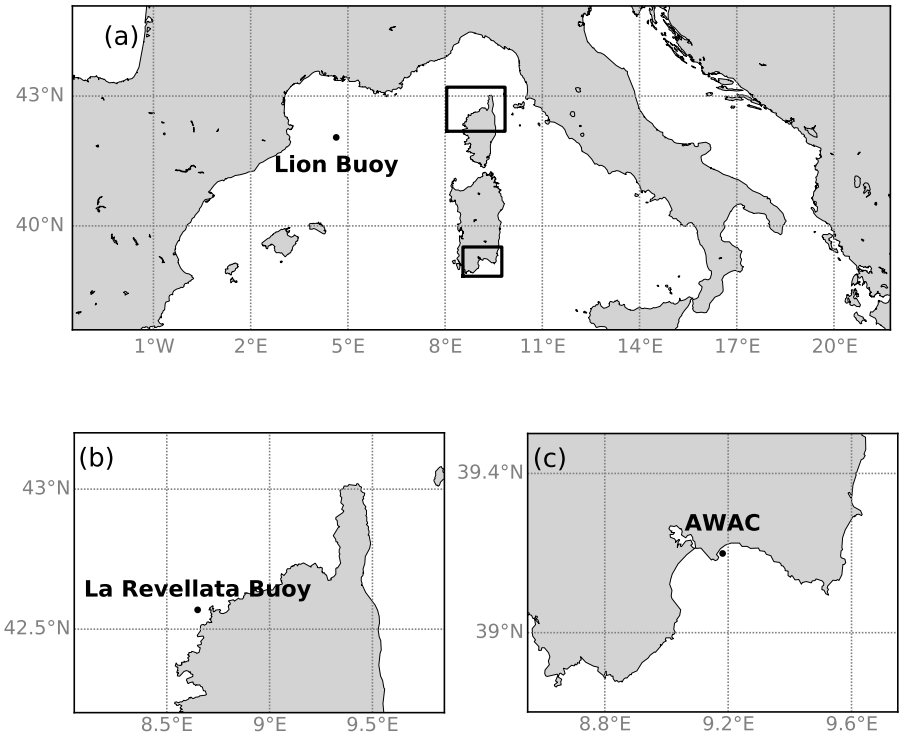

Figure 2. Geographic setting. (**a**) Western Mediterranean Sea; (**b**) Northern Corsica; (**c**) Southern Sardinia. The black dots indicate the location of the wave devices.

2.4. Operational Wave System

The operational system runs once a day to predict the wave evolution in the entire Mediterranean basin for 5 days ahead. This system includes the coupling of an atmospheric model with a wave propagation model.

The atmospheric evolution is predicted by the Global Forecast System (GFS) run by the National Center for Environmental Prediction (NCEP). The GFS is a numerical model that simulates the development of the atmosphere surrounding the entire terrestrial globe. NCEP runs the model every 6 h providing the full range of physical variables (such as temperature, pressure, wind speed, cloud cover, precipitation, etc.) that drive and characterize the atmospheric evolution up to 16 days in advance. The GFS model is set up with an horizontal spatial resolution of 0.25° (∼27 km at Mediterranean latitudes) whereas, in the vertical direction, the atmosphere is divided into 64 layers. The model output is setup with a time step of 3 h.

In the operational system, the wind field computed by the GFS model represents the forcing for the WaveWatch III (WWIII) wave model [27]. The WWIII model is run once a day and is set up to predict the wave evolution up to 5 days in advance with a time step of 3 h. WWIII is a depth-averaged and phase-averaged numerical model able to simulate the entire set of processes involved in the propagation of sea wave energy, from its generation in deep waters up to its dissipation in shallow waters. This makes WWIII computationally efficient and thus particularly suitable for wave simulations over large spatial domains such as those of ocean basins characterized by a wide range of water depths [28,29]. Moreover, the inclusion of shallow water physics packages in the recent versions of WWIII (such as version 4.18 used in this work) has extended the field of application of this model towards coastal waters. At the same time, it is worth mentioning the limit of WWIII in simulating the wave propagation pattern induced by the diffraction process around small islands [30] or artificial structures [31,32]. However, since diffraction is not expected to significantly affect wave propagation within the shoreface of Poetto beach, the use of WWIII in coastal waters appears justified in this study.

With the main purpose of simulating wave processes with different spatial scales, we adopt a multi-grid approach in which a large grid with a spatial resolution of 0.167° (∼18 km) extends over the entire Mediterranean basin, and a fine grid with a spatial resolution of 0.017° (∼1.8 km) covers the coastal seas surrounding the islands of Sardinia and Corsica. The fine grid extends over a region between the shoreline and 22 km offshore where boundary conditions are imposed accordingly to the wave field computed over the coarse grid. To avoid pronounced grid-boundary concavities located at the middle of large gulfs, the grid width extension is increased in these areas (see the panel (b) of Figure 3 that plots the grid configuration in the Gulf of Cagliari). Both coarse and fine grid simulations run over the bathymetry obtained using the ETOPO1 (Earth topography 1 arc minute) dataset [33]. The wave model is set up with 24 frequency bins and 24 directions. The frequency range covers from 0.04 to 0.74 Hz, whereas wave directions are 15° spaced. Nonlinear wave interactions in deep waters were computed with the Discrete Interaction Approximation method [34]. Triad wave interactions, accounting for nonlinear wave processes in intermediate and shallow waters, are also included. Table 1 lists the parameterizations used for the main source terms, see the WWIII manual [35] for an exhaustive explanation of the source terms.

Table 1. Source term treatment in WWIII.

	$S_{in} + S_{ds}$	S_{nl}	S_{bot}	S_{db}	S_{bs}	S_{tr}
Parameterizazion	ST4	NL1	BT4	DB1	BS1	TR1

During the period of the field experiment, wave model simulations started every morning once the first daily GFS simulation had been made available by NCEP. As initial condition, the model uses a restart file from the simulation of the previous day. The simulations are 117 h long from 00:00 of the first day until 21:00 of the fifth day. Under the current configuration, the multi-grid simulations run in

parallel using 2 cores (2.6 GHz) with an average simulation rate close to 90 simulated hours per hour. The output parameters, requested at intervals of three hours, are provided across both the large scale and small scale grids and at the points corresponding to the locations of the Lion buoy, La Revellata buoy and the AWAC. We examine in this paper the following parameters: wind speed at 10 m above the mean sea level U_{10}, significant wave height H_s, peak wave period T_p, mean wave period T_m, mean wave direction θ_m, wave direction at spectral peak θ_p, wave directional spread σ and full 2D wave spectrum $E(f,\theta)$. The comparison between simulations and measurements is carried out by means of single point statistical indicators such as correlation coefficient R, bias B, normalized root mean square error $RMSE$, relative error $RelE$ and scatter index SI. They are defined as:

$$R = \frac{\sum_{i=1}^{N}(M_i - \overline{M})(O_i - \overline{O})}{\sqrt{\sum_{i=1}^{N}(M_i - \overline{M})^2 \sum_{i=1}^{N}(O_i - \overline{O})^2}}, \quad (1)$$

$$B = \frac{1}{N}\sum_{i=1}^{N}(M_i - O_i), \quad (2)$$

$$RelE = \frac{1}{N}\sum_{i=1}^{N}\left|\frac{M_i - O_i}{O_i}\right|, \quad (3)$$

$$RMSE = \sqrt{\frac{1}{N}\sum_{i=1}^{N}(M_i - O_i)^2}, \quad (4)$$

$$SI = \frac{RMSE}{\overline{O}}, \quad (5)$$

where N is the number of measurements, M is the model result, O is the observation and the overbar indicates the sample mean.

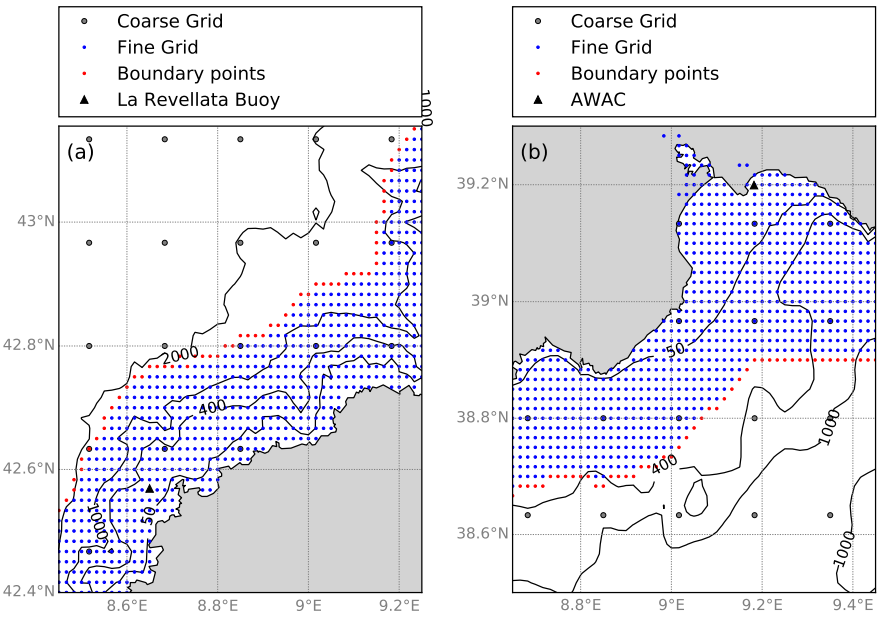

Figure 3. Details of computational grids. (**a**) Corsica; (**b**) Gulf of Cagliari. Thick lines are the coastline, thin lines represent the isobaths.

3. Results

Figures 4 and 5 show the comparison between measured and computed data of significant wave height H_s at the Lion buoy (deep water), La Revellata buoy (intermediate water) and AWAC (nearshore)

at Poetto. Comparisons of wind data time series are displayed in Figure 6. Wind measurements are extrapolated to an elevation equal to that of the GFS output (10 m above the mean sea level) by assuming that a logarithmic velocity profile develops within the atmospheric boundary layer:

$$\frac{U_z}{U_{10}} = 1 + \frac{C^{0.5}}{0.4} ln(\frac{z}{10}), \quad (6)$$

$$C = 0.001(0.067U_{10} + 0.75), \quad (7)$$

where U_{10} is the wind speed at 10 m above the mean sea level, C is a friction coefficient obtained with the formulation proposed by Garratt [36]. The statistical indicators of parameters displayed in Figures 5 and 6 are reported in Table 2. The operational wave system is able to satisfactorily reproduce the evolution of the significant wave height in deep/intermediate waters where the relative error is 17% both at Lion and La Revellata buoys. In addition, the wind evolution is well addressed by the GFS with a relative error (15%) on the same order of magnitude as that of significant wave height at the Lion buoy. Positive bias values suggest that both the predicted wind speed and wave height are slightly overestimated in deep waters. On the other hand, small negative bias values are observed at La Revellata buoy. The correlation coefficients of both wind and significant wave height (0.61 and 0.84) at Poetto beach are lower than those obtained in deep waters (0.91 and 0.93). The relative error of significant wave height exceeding 25% is likely to be related to the inaccuracies in wind speed predictions (relative error of 34%). In contrast with deep waters, nearshore data at Poetto beach are characterized by a pronounced short-period variability with daily peaks in wind speed and significant wave height possibly due to sea breezes (see Section 4). Although the system reproduces the general wind pattern, some peaks in wind speed are underestimated; see for instance the days following 24 April in which the anemometer measured wind speeds on the order of 20 kts but the GFS predicts speeds lower than 15 kts. As a result, significant wave heights during the same week are underestimated (although with less discrepancies than wind) by the wave model.

Table 2. Results of statistical analysis of spectral bulk wave parameters and wind speed U_{10} at Lion buoy, La Revellata buoy (only wave data) and Poetto locations.

	$\overline{O}$	R	B	$RMSE$	$RelE$	SI
Lion H_s	1.34 m	0.93	0.16 m	0.35 m	0.17	0.21
Lion U_{10}	15.82 kts	0.91	0.40 kts	2.98 kts	0.15	0.16
La Revellata H_s	1.00 m	0.91	−0.12 m	0.29 m	0.17	0.23
La Revellata T_m	4.33 s	0.84	0.02 s	0.75 s	0.14	0.17
La Revellata T_p	5.87 s	0.73	−0.09 s	1.16 s	0.14	0.20
La Revellata σ	38.11°	0.24	−7.53°	15.29 °	0.30	0.40
Poetto H_s	0.35 m	0.85	0.00 m	0.14 m	0.28	0.34
Poetto T_m	2.97 s	0.77	0.35 s	0.90 s	0.22	0.30
Poetto T_p	5.16 s	0.50	−0.34 s	1.93 s	0.27	0.34
Poetto σ	56.59°	0.49	−24.98°	29.81°	0.46	0.53
Poetto U_{10}	9.28 kts	0.62	−1.77 kts	4.27 kts	0.34	0.40

Figures 7 and 8 plot the time series of measured and predicted bulk wave parameters at La Revellata buoy and in the nearshore at the AWAC location, respectively. The evolution of significant wave height, already presented in Figure 5, is kept here as a reference. La Revellata buoy (Figure 7) measured maximum values of the mean period between 6 and 7 s while the peak period reached 10 s under energetic conditions. The model is able to satisfactorily catch the time evolution of mean and peak period ($relE$ of both mean and peak period is 0.14 with absolute B values lower than 0.1 s). The mean wave direction of propagation ranges from West-South-West to North and seems well reproduced by the model. The wave directional spread evolution is poorly caught by the model ($RelE = 0.30$) that, in addition, significantly underestimate its values ($B = -7.53°$).

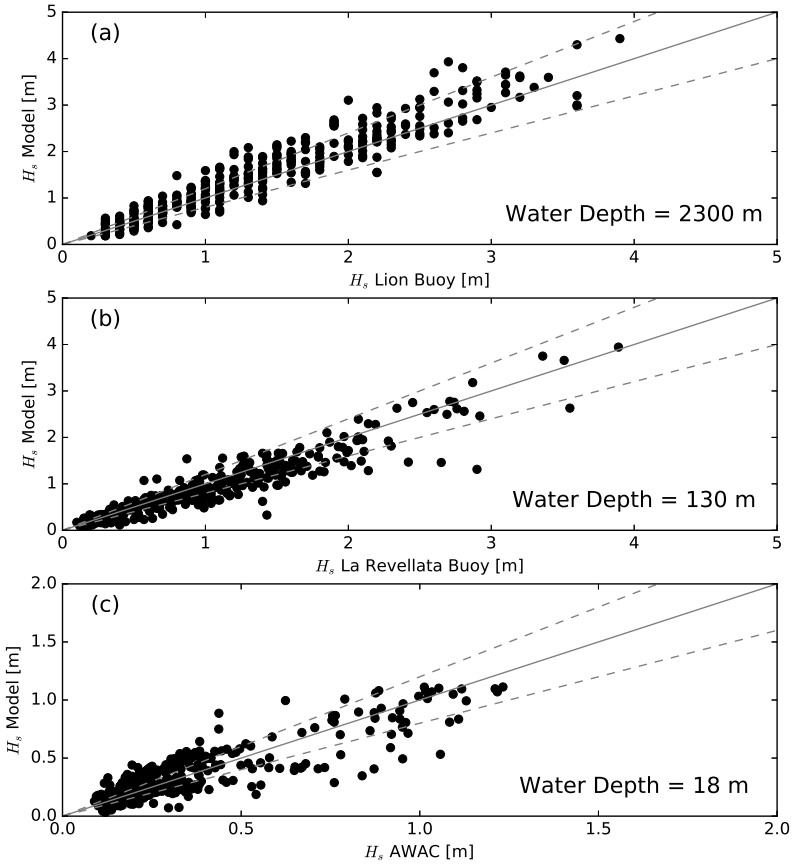

Figure 4. Scatter plots of computed versus observed H_S for the period of the experiment (from 31 March to 15 May 2017). (**a**) Lion buoy; (**b**) La Revellata; (**c**) AWAC at Poetto beach. Solid line, perfect agreement; dashed line, 20% error bound.

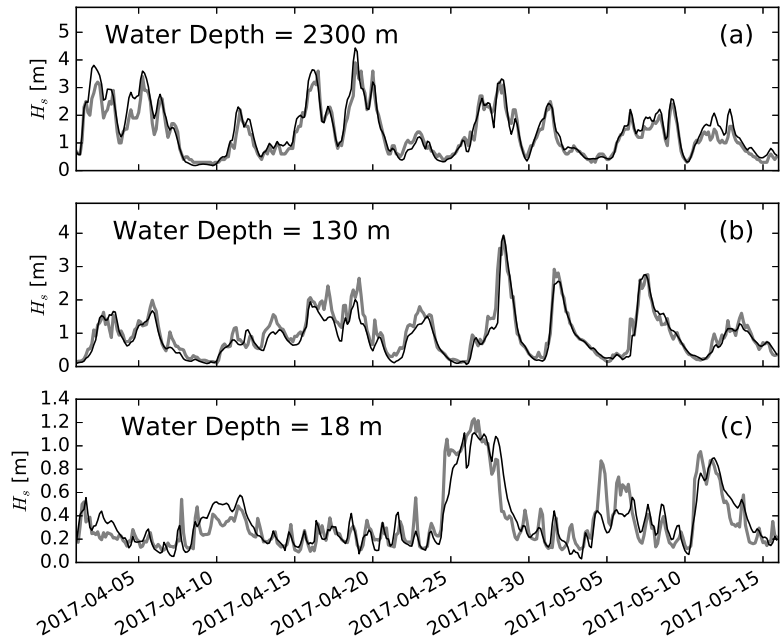

Figure 5. Comparisons between predictions and measurements of H_s time series at Lion buoy (**a**), La Revellata buoy (**b**) and AWAC at the Poetto beach (**c**). Thick gray line: observations; thin black line: predictions.

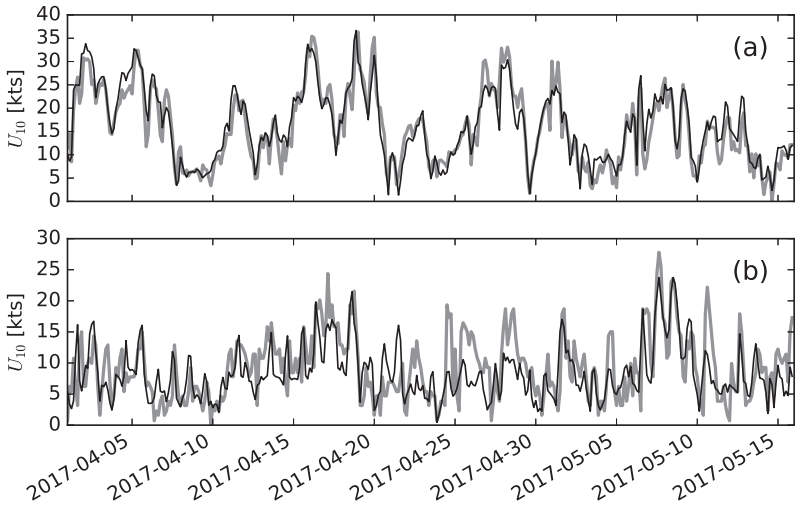

Figure 6. Comparisons between predictions and measurements of wind speed U_{10} time series at Lion buoy (**a**) and at the Poetto beach (**b**). Thick gray line: observations; thin black line: predictions.

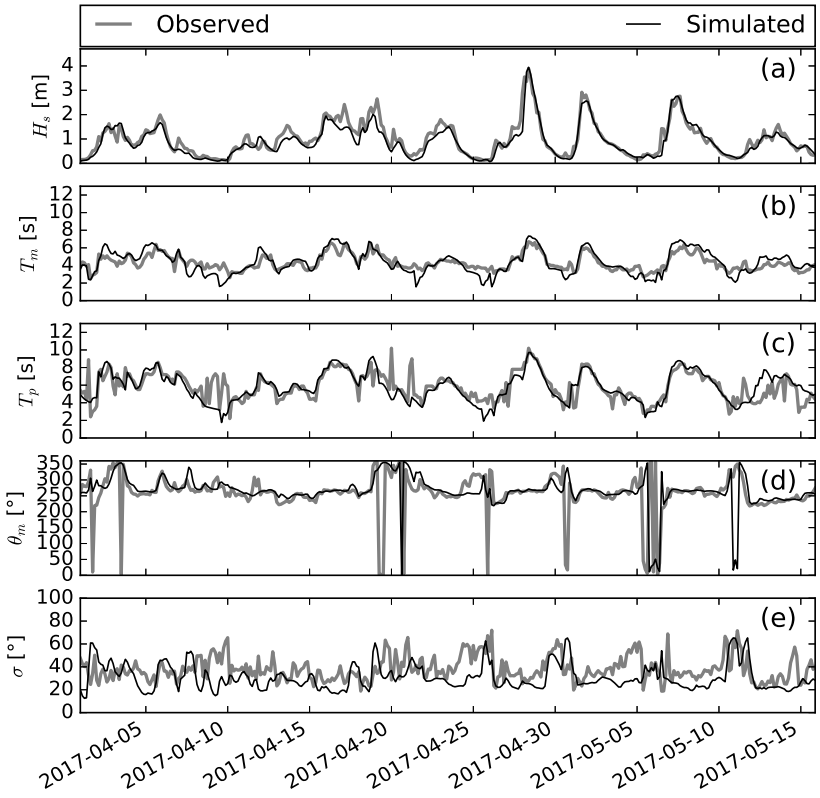

Figure 7. Comparisons between measurements and predictions of spectral bulk wave parameters at La Revellata buoy. H_s: significant wave height (**a**); T_m: mean period (**b**); T_p: peak period (**c**); θ_m: mean wave direction (**d**); σ: wave directional spread (**e**).

In coastal water at Poetto beach (Figure 8), mean periods (panel b) rise to values on the order of 5 and 6 s during relatively energetic conditions. At the same time, the peak period (panel c) reaches 7 to 8 s under energetic wave states with some abrupt variations due to shifts of the spectrum peak between sea and swell bands. While the wave model seems to correctly address the peak period maximum values ($relE$ = 0.27, bias B is -0.34 s), the mean period remains overestimated especially under energetic conditions ($relE$ = 0.22, $B = 0.35$ s). We will comment about this later in Section 4. The AWAC recorded incident waves with a mean direction of propagation ranging almost exclusively

between East and South-East. On the other hand, the mean wave direction predicted by the model tends to be more South and South-East with some notable inversions to offshore propagation. These inversions with waves coming from the North-West are noticeable also in the measured peak wave direction and are likely to be associated with offshore winds, weak incoming wave energies and small wave periods. Panel (f) of Figure 8 shows that the system significantly underestimates the values of the wave directional spread in nearshore waters (bias $B = -25°$). Large directional spread values on the order of 80° are recorded when peak wave direction turns to North-West (see panel e) implying the superposition of offshore and onshore propagating spectral components. In addition, the system predicts directional spread values in phase with offshore peak wave directions but with values hardly exceeding 60°. Besides the discrepancies in magnitude, the system is able to catch the main trend of directional spread variation with low values appearing when the mean wave direction is mainly South-East oriented (onshore).

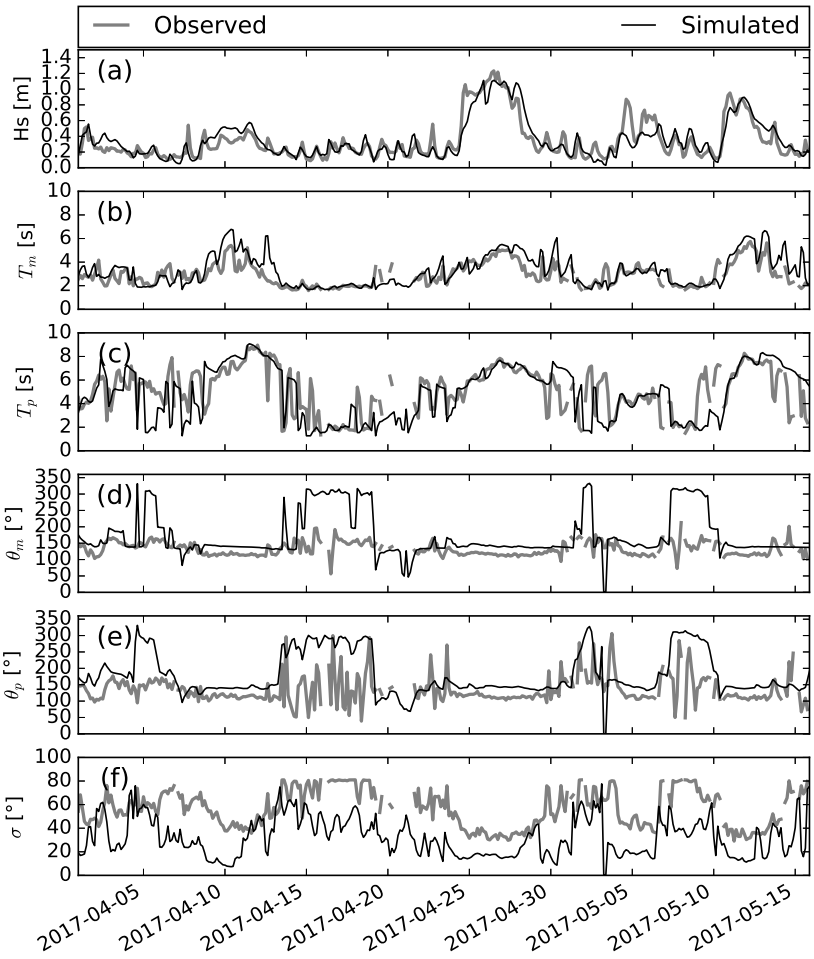

Figure 8. Comparisons between measurements and predictions of spectral bulk wave parameters at Poetto beach. H_s: significant wave height (**a**); T_m: mean period (**b**); T_p: peak period (**c**); θ_m: mean wave direction (**d**); θ_p: peak wave direction (**e**); σ: wave directional spread (**f**).

Although the operational wave system gives a prediction five days ahead, up to this point this work has made the assessment of the results for the first day of prediction only (with a temporal extension from 0 to 21 h from the beginning of the simulation). The quality of the prediction is expected to decrease as the time from the start of the simulation (lead-time) increases [6]. Figure 9 shows how the relative error at the Lion buoy rises from 17% of the first day to 27% of the fourth day of simulation (from 72 to 93 h from the start). Under the same lead-time range, the relative error passes from 17 to 28% at La Revellata buoy and from 28 to 35% at Poetto beach. This deterioration of the wave

forecast accuracy with the lead-time is likely to be related to larger uncertainties in the wind forcing fields [10,37]. Despite the accuracy loss, the relative error remains under moderate values, confirming the reliability of the prediction for the time window covered by the simulation. The bias B values at the three locations keep the same sign (positive at Lion buoy and negative at la Revellata) along the days of the time window without showing a clear trend. The analysis of the prediction accuracy as a function of lead-time is not further pursued in this work.

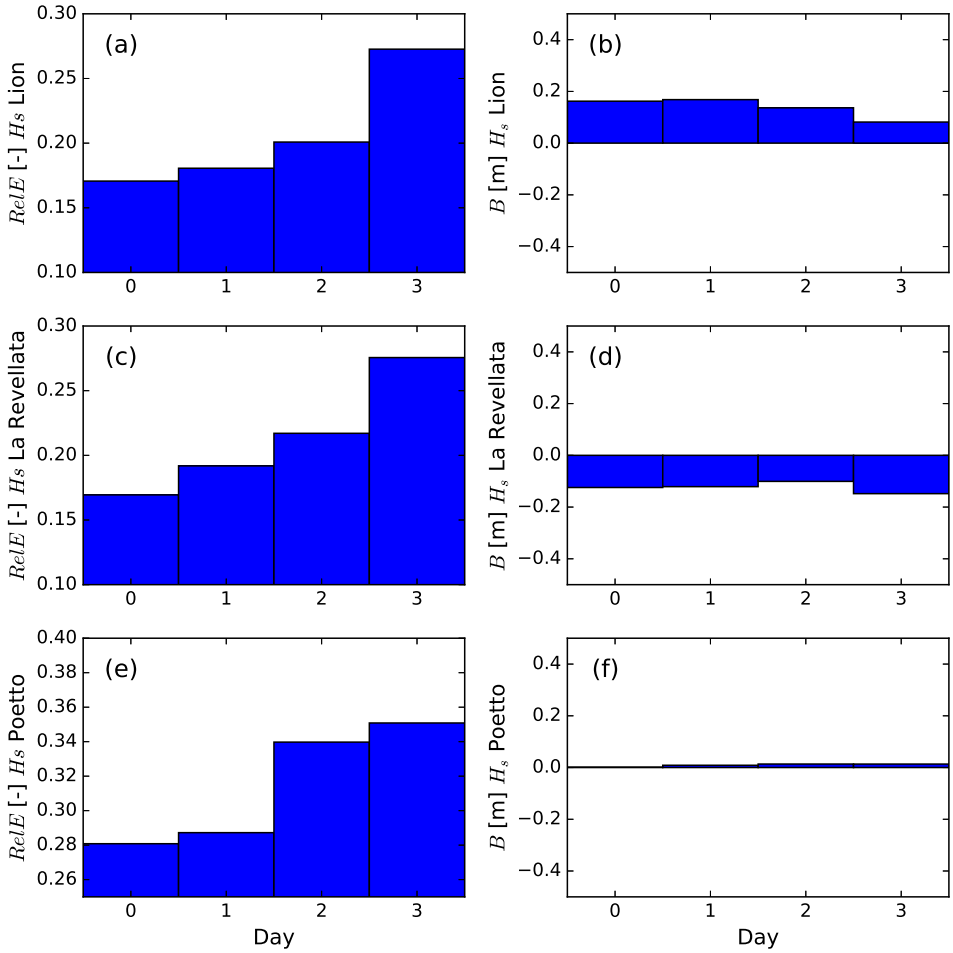

Figure 9. Performance of the operational wave system over the time window of the prediction. Relative error of significant wave height H_s versus day from the start of the simulation at Lion buoy (**a**), La Revellata buoy (**c**) and Poetto (**e**). Bias of H_s versus day from the start of the simulation at Lion buoy (**b**), La Revellata buoy (**d**) and Poetto (**f**).

4. Discussion

The results presented in Section 3 show that the operational wave system performs better in deep waters and intermediate waters than in the nearshore. This outcome is in agreement with Ravdas et al. [10] who found relatively low correlations at coastal locations. Whereas correlation coefficients for wind speed and significant wave height are 0.91 and 0.93 in deep waters at the Lion buoy site, they drop to 0.62 and 0.85 when computed data are compared with measurements in the nearshore at Poetto beach. The fact that in the nearshore the correlation coefficient of significant wave height is larger than that of the wind speed suggests that local meteorological forcing, playing an important role in wave dynamics, are not completely addressed by the GFS model. The GFS is a global meteorological model that, due to the adopted horizontal resolution (0.25°), may not be the most appropriate tool for forecasting coastal wind dynamics. Besides the fact that complex land

topographies play a significant role in the evolution of coastal winds, it is worth mentioning that it is in the spring season that the difference between the sea water temperature and the temperature of the lower layers of the atmosphere is strongest. This leads to intense coastal sea breezes blowing onshore at the central part of the day, resulting in marked daily oscillations in the wind speed and consequently in the significant wave height signals (see Figures 5 and 6). These factors together make the prediction of waves in coastal waters particularly challenging, especially in the spring season.

To investigate where the mentioned discrepancies in spectral bulk wave parameters come from, Figure 10 displays the observed and computed 2D wave spectra in the nearshore at the time instant of the maximum significant wave height recorded during the period of the experiment (see panel d). 1D frequency spectra are shown in the panel (c) of the Figure. The operational system predicts wave conditions with a mean propagation direction more southern oriented with respect to measurements (142° predicted versus 115° measured). This discrepancy is likely to be related to complex coastal bottom features leading to significant refraction processes that cannot be completely addressed even with the adoption of the small scale numerical grid. In fact, the spatial resolution of the fine grid (0.017°) seems to be able to address the main features of the wave propagation pattern in the nearshore but is likely to be unable to catch the detailed wave transformation in shallow waters. The use of a finer grid, proceeding from a detailed bathymetric survey, with a spatial resolution of the order of 100 m is expected to improve the characterization of nearshore and shallow water waves. However, one should bear in mind that this different set-up would bring a drawback represented by an increase of the computational cost. Due to the large number of different strategies and configuration settings that can be adopted to increase the characterization of coastal wave processes, we avoid providing here a quantitative estimation of the required increase of the computational effort.

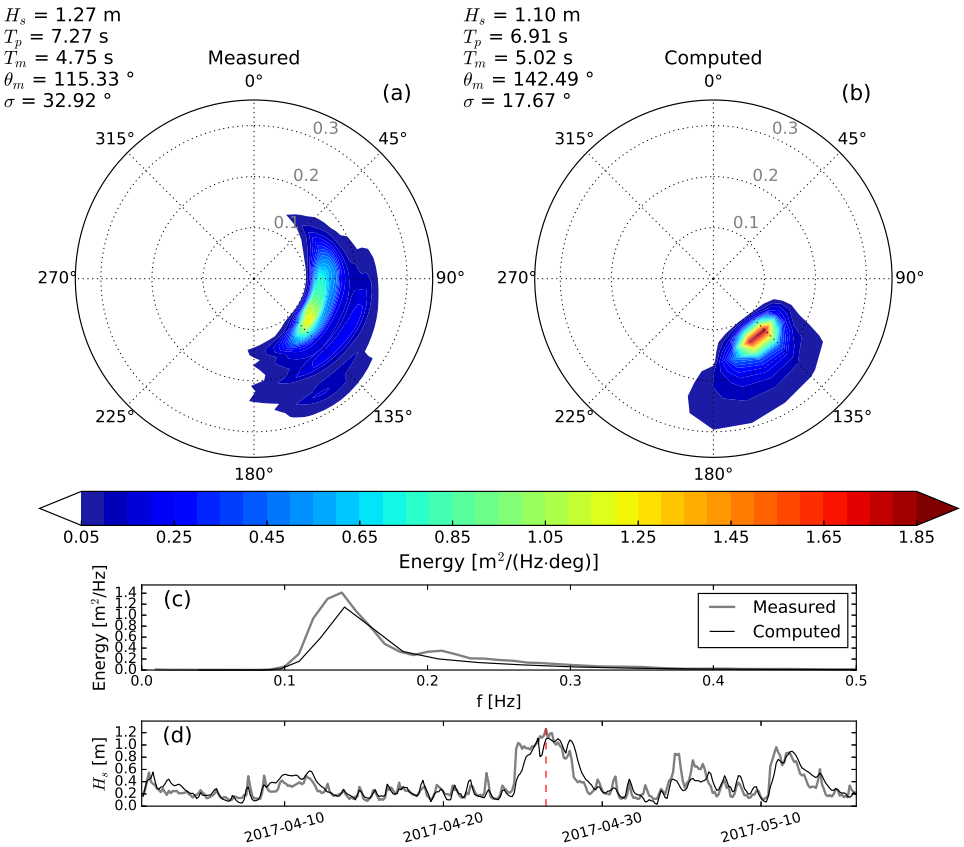

Figure 10. Measured (**a**) and predicted (**b**) two-dimensional wave spectra at the time instant of the measured maximum H_s. One-dimensional frequency spectra are plotted in panel (**c**). Panel (**d**) displays the time series of H_s. The time instant of the measured maximum H_s is highlighted by a dashed red line in panel (**d**).

From the observation of Figure 10, it is evident how wave energy is spread across a wide range of directions in the observed spectrum whereas computed energy tends to be concentrated around the main peak (simulated wave directional spread is 17.67° whereas the AWAC registered a direction spread of 32.92°). Negative biases in directional spread predictions have been reported by Crosby et al. [38] who ascribed this discrepancy to a weak computed coastal reflection. In our case, the spectral shape suggests that the directional spread underestimation is likely to be a consequence of the wind underestimation by the GFS model. In fact, Figure 6 reveals a significant underestimation of wind speed at Poetto when the maximum wave height occurs (morning of 26 April). Note also that the computed 1D spectrum lacks the secondary peak at 0.21 Hz that is clearly observable in the measurements (Figure 10, panel c). The underestimation of locally generated sea waves is likely to be responsible for the overestimation of the mean period. Since the wave results rely upon wind predictions, the use of a more accurate atmospheric model with a resolution able to address the effects induced by complex coastal topographies is expected to improve the characterization of sea wave components mainly driven by local meteorological forcing.

Relevant insight into the capability of the model to simulate nearshore wave processes can be achieved by the observation of Figure 11 that plots the time evolution of the measured and computed 1D frequency spectra at Poetto beach. Although discrepancies can be detected, the model satisfactorily reproduces the main evolution patterns of observed frequency spectra. In particular, moderate wave energy at high frequencies that appears in the period with absence of ground swells (see the period from 15 April 2017 to 23 April 2017) is likely to be generated by local wind breezes that blow over a limited fetch. In addition, the distribution of wave energy during the energetic events seems to be well addressed by the model, although the observation of panel (d) reveals that energy tends to be overpredicted at frequencies below the peak frequency. An analogous discrepancy was reported by Rogers and Vledder [39] who suggested that such overprediction is a common feature of models that implement the Discrete Interaction Approximation (DIA). Finally, the underprediction of high frequency energy is likely to be the result of the poor characterization of wind speed in coastal areas already mentioned.

The magnitude of the statistical error indicators of significant wave height found in the present study in intermediate and deep waters is on the same order of magnitude of that obtained by state-of-the-art wave systems recently developed for the Mediterranean basin [2,10]. In particular, Ravdas et al. [10] reported an averaged scatter index of 0.25 similar to the scatter index we obtained at La Revellata buoy (0.23). In that study, they compared the results of the operation wave system, based on the community Wave Model (WAM) forced by forecast winds from the European Centre for Medium-Range Weather Forecasts (ECMWF), with measured wave data proceeding from regional and national wave buoy nets deployed in water depths in the order of, or larger than, 100 m. Due to extensive measured dataset, they were able to provide assessment metrics for different Mediterranean Sea subregions. In contrast with the methodology followed by Ravdas et al. [10] who applied a computational grid with constant spatial resolution of 1/24° covering the whole Mediterranean basin, in this study we have nested a coastal fine grid (resolution 1/60°) into a deep-water coarse grid (resolution 1/6°). Our multi-grid approach is intended to improve the characterization of the coastal wave processes relevant for the beach monitoring program.

While most of the wave operational systems present in the literature are tested against data (from wave riders or satellite) retrieved in deep or intermediate water [2,6,10], we include an evaluation of our operational wave system against wave measurements collected at 18 m depth. Among the few examples of operational wave systems tested in shallow waters, we can compare our results with Ponce de Leon and Orfila [11]. Ponce de Leon and Orfila [11] used three different wind datasets and two phase-averaged spectral wave models with a grid resolution of 1500 m to simulate waves around Mallorca Island (Spain, Mediterranean Sea) under the effect of fast-changing sea breezes. Thus, their wave conditions, characterized by a combination of moderate Mediterranean swells and locally-generated wind waves, were similar to those we have observed in our experiment at Poetto

beach. Testing their system with wave data at a water depth of 135 m, they obtained a scatter index (SI = 0.35) higher than that we have obtained at the same depth (SI = 0.23 at La Revellata). However, when the evaluation was extended to shallower depths (28 m depth), the performance of their system decreased (SI = 0.4). A decrease in precision in shallower depths is also found in our work, but the SI for the system presented in this paper remains below 0.35. Although the quality of the predictions in coastal waters is not as excellent as that in intermediate and deep waters, the multi-grid approach adopted in this study allows the specification of the main wave propagation features in the presence of complex shoreline geometries and under the effect of coastal breezes.

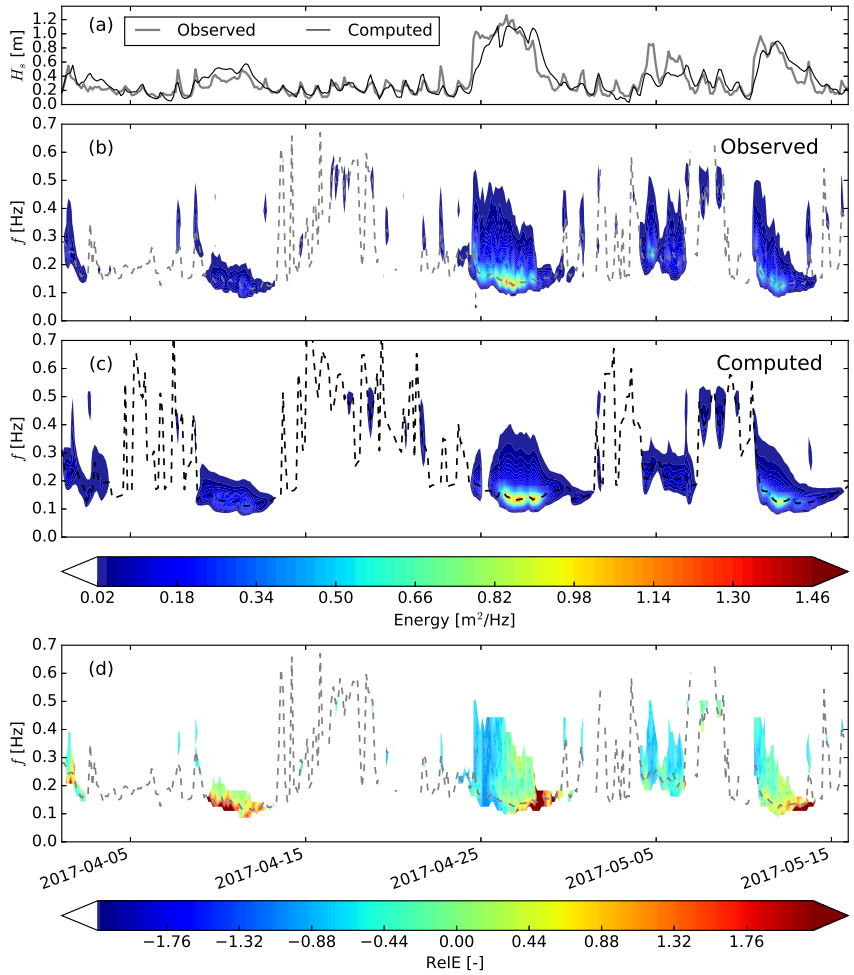

Figure 11. Temporal variation of 1D frequency spectra. (**a**) H_s time series. (**b**) Observed frequency spectra. (**c**) Computed frequency spectra. (**d**) Relative error of spectral energy density. Grey and black dashed lines are, respectively, the observed and computed peak frequency.

5. Conclusions

This work assesses the performance of an operational wave system included in a beach monitoring program for the Poetto beach (Southern Sardinia). The operational wave system aims to extend and complement in situ observations and the information collected by a video camera installation. The wind field from the atmospheric model GFS represents the forcing of the wave model WWIII. The wave model runs once a day to predict the wave evolution for five days ahead in the entire Mediterranean Sea using a multi-grid approach in which high spatial resolution is achieved in the coastal seas surrounding the islands of Sardinia and Corsica. The reliability of the operational system is tested by comparing the computed results with measurements collected at different water depths.

In general terms, the operational wave system presented in this work is able to predict the wave evolution in deep and intermediate waters with excellent accuracy (relative error of significant wave height is equal to 17%). However, the relative error of significant wave height rises to 28% in front of Poetto beach at 18 m depth. Moreover, the model underestimates the directional spread, especially in the nearshore (the bias is -8° in 130 m depth and -25° at 18 m depth). The analysis of spectral results suggest that the implementation of few improvements is advisable to refine the characterization of wave transformation processes in coastal and shallow waters. The main improvements can be identified as: an increased resolution of the computational grid (built from a detailed bathymetric survey) in coastal areas and the coupling with an atmospheric model able to catch local effects. These changes in the system configuration would have the associated drawback represented by an increase of the computational cost. Reducing the error in coastal waters would contribute to the reduction of the uncertainty of the operational wave system applications in coastal hazard and management.

Even with the mentioned limits, the information provided by the operational wave system can integrate measurements collected by in situ and remote systems inside a multi-platform monitoring program. By making this environmental dataset available to coastal scientists and managers, the monitoring program is of crucial importance to plan economical activities in coastal areas with applications including flood and erosion risk assessment, beach management and support to stakeholder activities. The dataset produced through the monitoring tasks is especially important in areas subject to considerable anthropological pressure, such as the beach systems of the metropolitan area of Cagliari, where the knowledge of wave forcing is a key factor to understand and predict short and long-term geomorphological processes.

Author Contributions: A.R. was responsible for the conceptualization, investigation and analysis; A.R. and C.B. wrote the original draft; M.P. and D.T. were responsible for the experimental methodology; A.I. and S.D.M. acquired funding and supervised the investigation; all authors reviewed and approved the manuscript; A.R. presented part of this work at the Coastlab 2018 conference.

Funding: This work was supported by: (1) Regione Autonoma Sardegna under L.R. 7/2007, "Promozione della ricerca scientifica e dell'innovazione tecnologica in Sardegna" for NEPTUNE and NEPTUNE 2 projects; (2) Consorzio di Bonifica Sardegna Meridionale (CBSM) under project number COM-CONV-2016DEMURO-CBSM-ARU.A.00.21. Marinella Passarella gratefully acknowledges Sardinia Regional Government for the financial support of her PhD scholarship (P.O.R. Sardegna F.S.E. Operational Programme of the Autonomous Region of Sardinia, European Social Fund 2007-2013 - Axis IV Human Resources, Objective l.3, Line of Activity l.3.1.). Daniele Trogu acknowledges the support by the University of Cagliari ("Borse di studio di Ateneo" - Dottorati di Ricerca XXXIV ciclo, voce CO.AN.A.06.01.01.01.01.02).

Acknowledgments: The authors would like to thank the Battellieri di Cagliari and Marco Piroddi for their assistance during the field campaign. Gilbert Emzivat of Meteo France and Alain Le Berre of CEREMA are acknowledged for providing the buoy data. The authors acknowledge the organizers of the Coastlab 2018 conference (22–26 May, Santander, Spain) where part of this research was first presented. The suggestions and comments made by the reviewers significantly improved the manuscript.

Conflicts of Interest: The authors declare no conflict of interest.

References

1. O'Reilly, W.; Olfe, C.B.; Thomas, J.; Seymour, R.; Guza, R. The California coastal wave monitoring and prediction system. *Coast. Eng.* **2016**, *116*, 118–132. [CrossRef]
2. Mentaschi, L.; Besio, G.; Cassola, F.; Mazzino, A. Performance evaluation of Wavewatch III in the Mediterranean Sea. *Ocean Model.* **2015**, *90*, 82–94. [CrossRef]
3. Sandhya, K.; Murty, P.; Deshmukh, A.N.; Nair, T.B.; Shenoi, S. An operational wave forecasting system for the east coast of India. *Estuar. Coast. Shelf Sci.* **2018**, *202*, 114–124. [CrossRef]
4. Sembiring, L.; van Ormondt, M.; van Dongeren, A.; Roelvink, D. A validation of an operational wave and surge prediction system for the Dutch coast. *Nat. Hazards Earth Syst. Sci.* **2015**, *15*, 1231–1242. [CrossRef]
5. Liberti, L.; Carillo, A.; Sannino, G. Wave energy resource assessment in the Mediterranean, the Italian perspective. *Renew. Energy* **2013**, *50*, 938–949. [CrossRef]

6. Gudes Soares, C.; Rusu, L.; Bernardino, M.; Pilar, P. An operational wave forecasting system for the Portuguese continental coastal area. *J. Oper. Oceanogr.* **2011**, *4*, 17–27. [CrossRef]
7. Brambilla, W.; van Rooijen, A.; Simeone, S.; Ibba, A.; De Muro, S. Field Observations, Video Monitoring and Numerical Modeling at Poetto Beach, Italy. *J. Coast. Res.* **2016**, *2*, 825–829. [CrossRef]
8. Atkinson, A.L.; Power, H.E.; Moura, T.; Hammond, T.; Callaghan, D.P.; Baldock, T.E. Assessment of runup predictions by empirical models on non-truncated beaches on the south-east Australian coast. *Coast. Eng.* **2017**, *119*, 15–31. [CrossRef]
9. Passarella, M.; Goldstein, E.B.; De Muro, S.; Coco, G. The use of genetic programming to develop a predictor of swash excursion on sandy beaches. *Nat. Hazards Earth Syst. Sci* **2018**, *18*, 599–611. [CrossRef]
10. Ravdas, M.; Zacharioudaki, A.; Korres, G. Implementation and validation of a new operational wave forecasting system of the Mediterranean Monitoring and Forecasting Centre in the framework of the Copernicus Marine Environment Monitoring Service. *Nat. Hazards Earth Syst. Sci.* **2018**, *18*, 2675–2695. [CrossRef]
11. Ponce de Leon, S.; Orfila, A. Numerical study of the marine breeze around Mallorca Island. *Appl. Ocean Res.* **2013**, *40*, 26–34. [CrossRef]
12. De Muro, S.; Porta, M.; Passarella, M.; Ibba, A. Geomorphology of four wave-dominated microtidal Mediterranean beach systems with Posidonia oceanica meadow: A case study of the Northern Sardinia coast. *J. Maps* **2017**, *13*, 74–85. [CrossRef]
13. De Muro, S.; Porta, M.; Pusceddu, N.; Frongia, P.; Passarella, M.; Ruju, A.; Buosi, C.; Ibba, A. Geomorphological processes of a Mediterranean urbanized beach (Sardinia, Gulf of Cagliari). *J. Maps* **2018**, *14*, 114–122. [CrossRef]
14. De Muro, S.; Ibba, A.; Simeone, S.; Buosi, C.; Brambilla, W. An integrated sea-land approach for mapping geomorphological and sedimentological features in an urban microtidal wave-dominated beach: a case study from S Sardinia, western Mediterranean. *J. Maps* **2017**, *13*, 822–835. [CrossRef]
15. Strazzera, E.; Cherchi, E.; Ferrini, S. *A* Choice Modelling Approach for Assessment of Use and Quasi-Option Values in Urban Planning for Areas of Environmental Interest; Sustainability Indicators and Environmental Valuation Working Papers 42903; Fondazione Eni Enrico Mattei (FEEM): Milano, Italy, 2008.
16. Buosi, C.; Cherchi, A.; Ibba, A.; Marras, B.; Marrucci, A.; Schintu, M. Benthic foraminiferal assemblages and sedimentological characterisation of the coastal system of the Cagliari area (southern Sardinia, Italy). *Boll. Soc. Paleontol. Ital.* **2013**, *52*, 1–9. [CrossRef]
17. Schintu, M.; Marrucci, A.; Marras, B.; Galgani, F.; Buosi, C.; Ibba, A.; Cherchi, A. Heavy metal accumulation in surface sediments at the port of Cagliari (Sardinia, western Mediterranean): Environmental assessment using sequential extractions and benthic foraminifera. *Mar. Pollut. Bull.* **2016**, *111*, 45–56. [CrossRef] [PubMed]
18. Simeone, S.; De falco, G.; Como, S.; Olita, A.; De Muro, S. Deposition dynamics of banquettes of Posidonia oceanica in beaches. *Rend. Online Soc. Geol. Ital.* **2008**, *3*, 726–727.
19. Vacchi, M.; De Falco, G.; Simeone, S.; Montefalcone, M.; Morri, C.; Ferrari, M.; Bianchi, C.N. Biogeomorphology of the Mediterranean Posidonia oceanica seagrass meadows. *Earth Surf. Process. Landf.* **2017**, *42*, 42–54. [CrossRef]
20. De Muro, S.; Pusceddu, N.; Buosi, C.; Ibba, A. Morphodynamics of a Mediterranean microtidal wave-dominated beach: Forms, processes and insights for coastal management. *J. Maps* **2017**, *13*, 26–36. [CrossRef]
21. Buosi, C.; Tecchiato, S.; Pusceddu, N.; Frongia, P.; Ibba, A.; De Muro, S. Geomorphology and sedimentology of Porto Pino, SW Sardinia, western Mediterranean. *J. Maps* **2017**, *13*, 470–485. [CrossRef]
22. Ruju, A.; Ibba, A.; Porta, M.; Buosi, C.; Passarella, M.; De Muro, S. The role of hydrodynamic forcing, sediment transport processes and bottom substratum in the shoreward development of Posidonia oceanica meadow. *Estuar. Coast. Shelf Sci.* **2018**, *212*, 63–72. [CrossRef]
23. Passarella, M. On the Prediction of Swash Excursion and the Role of Seagrass Beach-Cast Litter: Modelling and Observations. Ph.D. Thesis, University of Cagliari, Cagliari, Italy, 2019.
24. Holman, R.; Stanley, J. The history and technical capabilities of Argus. *Coast. Eng.* **2007**, *54*, 477–491. [CrossRef]
25. Kroon, A.; Davidson, M.; Aarninkhof, S.; Archetti, R.; Armaroli, C.; Gonzalez, M.; Medri, S.; Osorio, A.; Aagaard, T.; Holman, R.; Spanhoff, R. Application of remote sensing video systems to coastline management problems. *Coast. Eng.* **2007**, *54*, 493–505. [CrossRef]
26. Archetti, R.; Paci, A.; Carniel, S.; Bonaldo, D. Optimal index related to the shoreline dynamics during a storm: the case of Jesolo beach. *Nat. Hazards Earth Syst. Sci.* **2016**, *16*, 1107–1122. [CrossRef]

27. Tolman, H.L. A Third-Generation Model for Wind Waves on Slowly Varying, Unsteady, and Inhomogeneous Depths and Currents. *J. Phys. Oceanogr.* **1991**, *21*, 782–797. [CrossRef]
28. Besio, G.; Mentaschi, L.; Mazzino, A. Wave energy resource assessment in the Mediterranean Sea on the basis of a 35-year hindcast. *Energy* **2016**, *94*, 50–63. [CrossRef]
29. Perez, J.; Menendez, M.; Losada, I.J. GOW2: A global wave hindcast for coastal applications. *Coast. Eng.* **2017**, *124*, 1–11. [CrossRef]
30. Buosi, C.; Ibba, A.; Passarella, M.; Porta, M.; Ruju, A.; Trogu, D.; De Muro, S. Geomorphology, beach classification and seasonal morphodynamic transition of a Mediterranean gravel beach (Sardinia, Gulf of Cagliari). *J. Maps* **2019**. [CrossRef]
31. Ilic, S.; van der Westhuysen, A.; Roelvink, J.; Chadwick, A. Multidirectional wave transformation around detached breakwaters. *Coast. Eng.* **2007**, *54*, 775–789. [CrossRef]
32. Sartini, L.; Mentaschi, L.; Besio, G. Evaluating third generation wave spectral models performances in coastal areas. An application to Eastern Liguria. In Proceedings of the OCEANS 2015-Genova, Genoa, Italy, 18–21 May 2015; pp. 1–10.
33. Amante, C.; Eakins, B. *ETOPO1 1 Arc-Minute Global Relief Model: Procedures, Data Sources and Analysis*; Technical Report; NOAA Technical Memorandum NESDIS NGDC-24; NOAA, National Geophysical Data Center, Marine Geology and Geophysics Division: Boulder, CO, USA, 2009.
34. Hasselmann, S.; Hasselmann, K. Computations and Parameterizations of the Nonlinear Energy Transfer in a Gravity-Wave Spectrum. Part I: A New Method for Efficient Computations of the Exact Nonlinear Transfer Integral. *J. Phys. Oceanogr.* **1985**, *15*, 1369–1377. [CrossRef]
35. Tolman, H.L. *User Manual and System Documentation of WAVEWATCH III Version 4.18*; Technical Report; NOAA/NWS/NCEP: 5830 University Research Court, College Park, MD, USA, 2014.
36. Garratt, J.R. Review of Drag Coefficients over Oceans and Continents. *Mon. Weather Rev.* **1977**, *105*, 915–929. [CrossRef]
37. Bernier, N.B.; Alves, J.H.G.M.; Tolman, H.; Chawla, A.; Peel, S.; Pouliot, B.; Bélanger, J.M.; Pellerin, P.; Lépine, M.; Roch, M. Operational Wave Prediction System at Environment Canada: Going Global to Improve Regional Forecast Skill. *Weather Forecast.* **2016**, *31*, 353–370. [CrossRef]
38. Crosby, S.C.; O'Reilly, W.C.; Guza, R.T. Modeling Long-Period Swell in Southern California: Practical Boundary Conditions from Buoy Observations and Global Wave Model Predictions. *J. Atmos. Ocean. Technol.* **2016**, *33*, 1673–1690. [CrossRef]
39. Rogers, W.E.; Vledder, G.P.V. Frequency width in predictions of windsea spectra and the role of the nonlinear solver. *Ocean Model.* **2013**, *70*, 52–61. [CrossRef]